AIMS Mathematics, 11(3): 7155–7182.
DOI: 10.3934/math.2026295
Received: 14 January 2026
Revised: 09 March 2026
Accepted: 11 March 2026
Published: 18 March 2026

https://www.aimspress.com/journal/Math

Research article

Bifurcations and chaos control for a discrete fractional-order Leslie-Gower model incorporating fear in predators and Allee effect in prey

Abdulaziz Almaslokh[1,*], **Ibrahim M. E. Abdelstar**[2] **and A. A. Elsadany**[1]

[1] Department of Mathematics, Faculty of Sciences and Humanities in Al-Kharj, Prince Sattam bin Abdulaziz University, Al-Kharj 11942, Saudi Arabia

[2] Department of Mathematics, Faculty of Science, Al-Azhar University, Nasr City, P.O.Box: 11884, Cairo, Egypt

* **Correspondence:** Email: am.almaslokh@psau.edu.sa.

Abstract: In this research, we analyze a discrete-time fractional-order modified Leslie-Gower predator-prey model that incorporates the Allee effect on prey and the fear effect on predators. The findings demonstrate complex dynamic behaviors resulting from these elements. First, we show the existence of equilibrium points and the conditions for their stability. Moreover, the incorporation of Allee and fear effects leads to various bifurcations, such as Neimark-Sacker and flip bifurcations. We perform numerical simulations with different values of the fractional parameter q to illustrate the complex temporal dynamics of the model. The theoretical results are corroborated and confirmed through numerical simulations.

Keywords: Leslie-Gower predator-prey model; fractional-order; fear effect; Allee effect; Neimark-Sacker; flip bifurcations
Mathematics Subject Classification: 37N25, 37N30, 34D35, 34D05, 39A28, 39A30

1. Introduction

The predator-prey relationship is a fundamental interaction in ecological systems, describing how two species dynamically affect each other's population dynamics over time. Understanding these interactions is crucial for predicting ecosystems' stability, biodiversity conservation, and resource management. This class of models has garnered significant attention from researchers in mathematics and biology due to its theoretical richness and practical applications [1–4].

Traditional predator-prey theory often assumes that predator populations depend entirely on the consumption of prey. Nevertheless, the ecological reality is more intricate. The Leslie-Gower model enhances these dynamics by correlating the predator's carrying capacity with the prey's availability,

acknowledging that predators' expansion is limited by this environmental constraint. In contrast to the Lotka-Volterra model, which posits that predator's growth is directly proportionate to the prey's availability, this approach incorporates a more realistic limitation: The predator population's growth is constrained by the prey population's ability to sustain it. This illustrates biological reality, like energy requirements, territorial behavior, and prey quality, thus averting false surges in predator populations. Subsequently, Aziz-Alaoui and Okiye [5] presented a revised Leslie-Gower model that incorporates predators' dietary flexibility, enabling them to survive periods of prey shortage by using other food sources. The model generally produces stable equilibria or constrained cycles, consistent with documented ecological dynamics in vertebrate and invertebrate systems. The Leslie-Gower paradigm has been used to examine interactions among parasitic insects and their hosts, avian predators, and small mammals, as well as marine predators whose reproductive success is significantly reliant on prey biomass [6, 7]. In order to investigate biological control strategies, ecosystems' resilience in the appearance of environmental stressors, and the factors that contribute to the stabilization of diversity or predator extinction, modified iterations of the model have been implemented [8, 9]. These iterations incorporate refuge effects, analogous dynamics, and nonlinear functional responses. This ecological model's discrete-time formulation is particularly well-suited for populations with non-overlapping generations or seasonal reproduction, in which population fluctuations occur at specified intervals. This can clarify irregular population oscillations by elucidating intricate dynamics such as flip and Neimark-Sacker bifurcations, invariant closed curves, and chaos. Additionally, the periodic nature of ecological time-series data renders discrete-time models particularly well-suited for the analysis of actual population dynamics.

Population dynamics are further complicated by the Allee effect, first described by Allee in the 1930s [10]. This phenomenon describes how individuals in low-density populations face reduced fitness due to difficulties in finding mates, cooperative defense, or foraging efficiency [11, 12]. Subsequently, researchers have identified various manifestations, including strong Allee effects [13], weak Allee effects [14], and multiple simultaneous Allee effects [15]. The incorporation of Allee effects in predator-prey models has revealed rich dynamic behaviors, including bifurcations and multiple attractors [15].

Beyond direct consumption, predators influence prey through non-lethal mechanisms. Prey species exhibit antipredator behavioral responses, altering their habitat use, foraging patterns, and vigilance levels in response to perceived threats. For example, birds may abandon nests [16], and mule deer reduce foraging time when cougars are present [17]. Recent research has revealed that such fear effects extend upward through food chains and can significantly impact an ecosystem's dynamics. Chen [18] examined the dynamic behaviors of a Leslie-Gower model with the Allee effect and fear effects, using blow-up methods to explore the stability of equilibrium points and determine conditions for Hopf bifurcation through first Lyapunov coefficient calculations. Wu and Xiong [19] studied the dynamics of a slow-fast modified Leslie-Gower model with a weak Allee effect and fear effects on predators, proving the existence of canard cycles and relaxation oscillations using geometric singular perturbation theory. This hierarchical fear effect underscores the importance of incorporating both direct and indirect predation effects in ecological models.

Building upon these ecological insights and recent developments in the field, this study examines a modified Leslie–Gower predator–prey model that incorporates the fear effect on predators and the strong Allee effect on prey [19] as follows:

$$\begin{aligned} \frac{dL}{dt} &= aL\,(1-L)\,(L-b) - cLG, \\ \frac{dG}{dt} &= \frac{G}{d+G}\left(1 - \frac{G}{e+L}\right), \end{aligned} \tag{1.1}$$

where L and G represent the densities of prey and predators at time t, respectively, with the initial conditions $L(0) = L_0 \geq 0$, $G(0) = G_0 \geq 0$. The parameters a, b, c, d, and e are positive constants.

The primary objective of this article is to extend the findings presented in [20] by formulating and analyzing a discrete-time fractional-order version of the model (1.1). Fractional calculus has emerged as a powerful mathematical framework for modeling biological systems because it naturally incorporates memory effects, a crucial feature of ecological interactions [21–23]. Among the various fractional derivative definitions [22, 24], the Caputo derivative is particularly suitable for biological applications, as it accommodates conventional initial conditions and yields zero for constant functions, enhancing its practical utility [25]. Researchers have successfully applied fractional-order models to diverse biological phenomena [26, 27], including predator-prey dynamics [28, 29]. Recent work by Rihan et al. [30] investigated a delayed Leslie–Gower fractional-order predator–prey model with fear effects and prey refuge, studying the nonnegativity, boundedness, and stability of equilibria, as well as conditions for Hopf bifurcation using time delay as a bifurcation parameter.
The fractional-order formulation of the model (1.1) in the Caputo sense is given by

$$\begin{aligned} D^q L(t) &= aL\,(1-L)\,(L-b) - cLG, \\ D^q G(t) &= \frac{G}{d+G}\left(1 - \frac{G}{e+L}\right), \end{aligned} \tag{1.2}$$

where D^q denotes the Caputo fractional derivative of order $q \in (0, 1)$. This fractional generalization offers advantages over traditional integer-order formulations, as it captures the memory-dependent and time-evolving nature of ecological interactions. For example, analogous fractional extensions have improved models of immune system responses to cancer by incorporating historically dependent behaviors that integer-order models cannot represent [31, 32].

The aim of this work is to further investigate the system's dynamics through the application of discretization techniques [33–35]. This approach allows us to examine how step size influences the system's stability and facilitates the observation of transitions from stable behavior to complex dynamics, including various types of bifurcations. Understanding these transitions provides a flexible framework for modulating the system's stability and improving the prediction of ecological outcomes. As highlighted in recent studies, bifurcation analysis in discrete-time systems reveals a range of rich dynamic phenomena, particularly codimension-1 bifurcations such as flip and Neimark-Sacker bifurcations, which are essential for understanding ecosystems' responses to parameter variations.

The remainder of this paper is organized as follows. Section 2 presents the discrete-time fractional-order formulation. Section 3 establishes conditions for the existence and uniqueness of the solution. Section 4 analyzes equilibrium stability, while Section 5 details criteria for flip, Neimark-Sacker, and combined bifurcations. Section 6 provides numerical simulations illustrating the theoretical findings, and Section 7 concludes with a discussion of the results.

2. Discretization process

The discretized variant offers distinct methodological advantages in the present ecological context. In numerous biological populations, reproduction occurs at various times of the year or between non-overlapping generations. This renders discrete-time models more realistic than their continuous counterparts. Furthermore, discrete systems can generate flip and Neimark-Sacker bifurcations, which are dynamic phenomena that are exclusive to discrete maps and that are absent in autonomous continuous-time models of equivalent size. This renders the framework ideal for examining the intricate oscillatory and chaotic dynamics observed in ecological time series. From a methodological perspective, discretization facilitates a direct comparison with data collected at fixed intervals and aids in the construction of bifurcation diagrams and an analysis of Lyapunov exponents [28, 36]. However, it is crucial to recognize their shortcomings: Discrete systems may exhibit heightened sensitivity to parameter variations, and their behavior in dynamic contexts can be contingent upon the chosen discretization scheme. Conversely, continuous-time formulations offer a more cohesive analytical framework. The discrete model is not intended to serve as an accurate representation of the continuous system. Rather, it is intended to serve as an independent illustration of generation-based dynamics. The discretization decision in this study is intentionally grounded in biological principles, rather than merely for the convenience of numerical representation.

Two-dimensional dynamic systems based on continuous-time fractional-order models are insufficient for characterizing chaotic phenomena. To address this, shifting to difference equations through discretization becomes necessary. Among the limited methodologies, utilizing piecewise constant arguments is notable for deriving an explicit difference equation from a fractional-order dynamic system [28,36,37]. Equations with piecewise constant arguments integrate the features of both differential and difference equations, facilitating the depiction of more intricate dynamical behaviors than their continuous counterparts. This study uses this technique to discretize the model (1.2). Therefore, we reconceptualize the model (1.2) as a collection of differential equations that integrate piecewise constant arguments, as detailed below.

$$\begin{aligned} D^q L(t) &= aL\left(\left[\frac{t}{h}\right]h\right)\left(1 - L\left(\left[\frac{t}{h}\right]h\right)\right)\left(L\left(\left[\frac{t}{h}\right]h\right) - b\right) - cL\left(\left[\frac{t}{h}\right]h\right)G\left(\left[\frac{t}{h}\right]h\right), \\ D^q G(t) &= \frac{G\left(\left[\frac{t}{h}\right]h\right)}{d + G\left(\left[\frac{t}{h}\right]h\right)}\left(1 - \frac{G\left(\left[\frac{t}{h}\right]h\right)}{e + L\left(\left[\frac{t}{h}\right]h\right)}\right), \end{aligned} \tag{2.1}$$

If $t \in [0, h)$ then, $\frac{t}{h} \in (0, 1)$. Therefore, we have

$$\begin{aligned} D^q L(t) &= aL_0\left(1 - L_0\right)\left(L_0 - b\right) - cL_0G_0, \\ D^q G(t) &= \frac{G_0}{d + G_0}\left(1 - \frac{G_0}{e + L_0}\right), \end{aligned} \tag{2.2}$$

and the solution (2.2) is derived as follows:

$$\begin{aligned} L_1(t) &= L_0 + I^q\left[aL_0\left(1 - L_0\right)\left(L_0 - b\right) - cL_0G_0\right], \\ G_1(t) &= G_0 + I^q\left[\frac{G_0}{d + G_0}\left(1 - \frac{G_0}{e + L_0}\right)\right]. \end{aligned} \tag{2.3}$$

Therefore,

$$\begin{aligned} L_1(t) &= L_0 + \frac{t^q}{\Gamma(1+q)}\left[aL_0(1-L_0)(L_0-b) - cL_0G_0\right], \\ G_1(t) &= G_0 + \frac{t^q}{\Gamma(1+q)}\left[\frac{G_0}{d+G_0}\left(1-\frac{G_0}{e+L_0}\right)\right]. \end{aligned} \tag{2.4}$$

If $t \in [h, 2h)$, then, $\frac{t}{h} \in (1, 2)$. Thus, we have

$$\begin{aligned} D^qL(t) &= aL_1(1-L_1)(L_1-b) - cL_1G_1, \\ D^qG(t) &= \frac{G_1}{d+G_1}\left(1-\frac{G_1}{e+L_1}\right), \end{aligned} \tag{2.5}$$

and the solution (2.5) is derived as follows:

$$\begin{aligned} L_2(t) &= L_1 + I^q\left[aL_1(1-L_1)(L_1-b) - cL_1G_1\right], \\ G_2(t) &= G_1 + I^q\left[\frac{G_1}{d+G_1}\left(1-\frac{G_1}{e+L_1}\right)\right]. \end{aligned} \tag{2.6}$$

In this case,

$$\begin{aligned} L_2(t) &= L_1 + \frac{t^q}{\Gamma(1+q)}\left[aL_1(1-L_1)(L_1-b) - cL_1G_1\right], \\ G_2(t) &= G_1 + \frac{t^q}{\Gamma(1+q)}\left[\frac{G_1}{d+G_1}\left(1-\frac{G_1}{e+L_1}\right)\right]. \end{aligned} \tag{2.7}$$

By repeating the process, the solution to (1.2) is derived as follows:

$$\begin{aligned} L_{(n+1)}(t) &= L_n(nh) + \frac{(t-nh)^q}{\Gamma(q+1)}\left[aL_n(nh)(1-L_n(nh))(L_n(nh)-b) - cL_n(nh)G_n(nh)\right], \\ G_{(n+1)}(t) &= G_n(nh) + \frac{(t-nh)^q}{\Gamma(q+1)}\left[\frac{G_n(nh)}{d+G_n(nh)}\left(1-\frac{G_n(nh)}{e+L_n(nh)}\right)\right]. \end{aligned} \tag{2.8}$$

Let $t = (n+1)h$; we then obtain

$$\begin{aligned} L_{(n+1)}((n+1)h) &= L_n(nh) + \frac{h^q}{\Gamma(q+1)}\left[aL_n(nh)(1-L_n(nh))(L_n(nh)-b) - cL_n(nh)G_n(nh)\right], \\ G_{(n+1)}((n+1)h) &= G_n(nh) + \frac{h^q}{\Gamma(q+1)}\left[\frac{G_n(nh)}{d+G_n(nh)}\left(1-\frac{G_n(nh)}{e+L_n(nh)}\right)\right], \end{aligned} \tag{2.9}$$

which leads to

$$\begin{aligned} L_{n+1} &= L_n + \frac{h^q}{\Gamma(q+1)}\left[aL_n(1-L_n)(L_n-b) - cL_nG_n\right], \\ G_{n+1} &= G_n + \frac{h^q}{\Gamma(q+1)}\left[\frac{G_n}{d+G_n}\left(1-\frac{G_n}{e+L_n}\right)\right]. \end{aligned} \tag{2.10}$$

3. Existence and uniqueness of the solution

This section is devoted to the study of the existence and uniqueness of solutions for the system (2.10).

Theorem 1. *The solution of the system* (2.10) *in the region* $\Psi \times (0, T]$ *with the initial conditions* $L(0) = L_0$ *and* $t \in (0, T]$ *is exist and unique if*

$$C = \frac{T^q}{\Gamma(1+q)} \max\left\{(3a+1)\theta^2 + ((2b+2)a - c)\theta - ab, (c-d)\theta + de - \theta^2\right\} < 1,$$

for some $\theta \in \mathbb{R}^+ < \infty$.

Proof. Equation (1.2) can be written as

$$D_t^q M(t) = N(M(t)), \quad t \in (0, T], \quad M(0) = M_0, \tag{3.1}$$

where

$$M = \begin{bmatrix} L \\ G \end{bmatrix}, \; M_0 = \begin{bmatrix} L_0 \\ G_0 \end{bmatrix}, \; N(M) = \begin{bmatrix} aL(1-L)(L-b) - cLG \\ \frac{G}{d+G}\left(1 - \frac{G}{e+L}\right), \end{bmatrix}.$$

Define

$$\|P\| = \sup_{t \in (0,T]} |P(t)|,$$

Then $M = \left[m_{ij}[t]\right]$ can be defined as

$$\|M\| = \max_i \sum_j m_{ij}[t].$$

Define the region $\Psi \times (0, T]$ where

$$\Psi = \{(L, G) : \max(|L|, |G|) \leq \theta\}. \tag{3.2}$$

Hence, the solution of the system (1.2) is given as follows

$$P = P_0 + \frac{1}{\Gamma(q)} \int_0^t (t-\tau)^{q-1} N(M(\tau))\, d\tau = Q(L).$$

Therefore

$$Q(M_1) - Q(M_2) = \frac{1}{\Gamma(q)} \int_0^t (t-\tau)^{q-1} [N(M_1(\tau)) - N(M_2(\tau))]\, d\tau. \tag{3.3}$$

We then have

$$\begin{aligned} |Q(M_1) - Q(M_2)| &\leq \frac{1}{\Gamma(q)} \int_0^t \left|(t-\tau)^{q-1} [N(M_1(\tau)) - N(M_2(\tau))]\right| d\tau, \\ &\leq \frac{1}{\Gamma(q)} \int_0^t \left|(t-\tau)^{q-1}\right| |N(M_1(\tau)) - N(M_2(\tau))|\, d\tau, \end{aligned} \tag{3.4}$$

and

$$\|Q(M_1) - Q(M_2)\| \leq \frac{T^q}{\Gamma(1+q)} \max\left\{(3a+1)\theta^2 + ((2b+2)a - c)\theta - ab, (c-d)\theta + de - \theta^2\right\}$$
$$. \|M_1 - M_2\| \leq C \|M_1 - M_2\|,$$

where

$$C = \frac{T^q}{\Gamma(1+q)} \max\left\{(3a+1)\theta^2 + ((2b+2)a - c)\theta - ab, (c-d)\theta + de - \theta^2\right\}.$$

If $C < 1$, then the mapping $L = Q(L)$ is a contraction mapping, and thus it is concluded that Theorem 1 is proved.

4. Dynamic behaviors of the discrete-time fractional-order Leslie-Gower system with fear effect in predator and strong Allee effect in prey

4.1. Stability analysis

Here, we study the stability analysis around the fixed points of the model (2.10).
To evaluate the equilibrium points of (2.10), let

$$L_{n+1} = L_n,\ G_{n+1} = G_n.$$

The discrete dynamic system (2.10) then has four equilibrium points, which are the following:

1. The Trivial equilibrium point $P_0 = (0, 0)$, which always exists;
2. the prey-free equilibrium point $P_1 = (0, e)$, which always exists;
3. the predator-free equilibrium $P_2 = (b, 0)$ and $P_3 = (1, 0)$ which always exists;
4. the coexistence equilibrium $P_* = (L_*, e + L_*)$, where L_* is the root of the following equation:

$$L_*^2 + (\frac{c}{a} - b - 1)L_* + b + \frac{ec}{a} = 0. \tag{4.1}$$

Clearly, the following possible results can be obtained.

(a) System (2.10) has no positive equilibrium in the following two cases:
   i. When $c = a(b+1)$;
   ii. when $e > \frac{a\left(\left(b+1-\frac{c}{a}\right)^2 - 4b\right)}{4c}$.

   In these two cases, (2.10) has complex roots.

(b) System (2.10) has only a positive equilibrium in the following two cases:
   i. At $e = \frac{a\left(\left(b+1-\frac{c}{a}\right)^2 - 4b\right)}{4c}$, model (2.10) has a positive equilibrium $P_4 = \left(\frac{a+ab-c}{2a}, e + \frac{a+ab-c}{2a}\right)$;
   ii. when $|a + ab - c| < a\sqrt{\Delta}$, model (2.10) has a positive equilibrium $P_5 = \left(\frac{a(1+b+\sqrt{\Delta})-c}{2a}, e + \frac{a(1+b+\sqrt{\Delta})-c}{2a}\right)$ (in this case, (2.10) has two real roots of opposite signs).

(c) At $\Delta > 0$ and $c < a\left(1 + b - \sqrt{\Delta}\right)$, the model (2.10) has two positive equilibria $P_6 = \left(\frac{a(1+b-\sqrt{\Delta})-c}{2a}, e + \frac{a(1+b-\sqrt{\Delta})-c}{2a}\right)$ and $P_7 = \left(\frac{a(1+b+\sqrt{\Delta})-c}{2a}, e + \frac{a(1+b+\sqrt{\Delta})-c}{2a}\right)$,

where $\Delta = (\frac{c}{a} - b - 1)^2 - 4\left(b + \frac{ec}{a}\right)$.

In our study of stability, we will focus on the points P_1, P_2, P_3, and P_6. This is because the point P_0 does not exist in real life, and analyzing P_3 is equivalent to studying P_2 by setting $b = 1$. Similarly, the points P_4 and P_6 can be analyzed in the same way as P_7.

The stability of the system's equilibrium points can be examined via the following theorems.

Lemma 1. *[38] Let $F(\xi) = \xi^2 + r\xi + s$. Suppose that $F(1) > 0$; ξ_1 and ξ_2 are the roots of $F(\xi) = 0$. We then have*

1. *$|\xi_1| < 1$ and $|\xi_2| < 1$ if and only if $F(-1) > 0$ and $s < 1$;*
2. *$|\xi_1| < 1$ and $|\xi_2| > 1$ (or $|\xi_1| > 1$ and $|\xi_2| < 1$) if and only if $F(-1) < 0$;*
3. *$|\xi_1| > 1$ and $|\xi_2| > 1$ if and only if $F(-1) > 0$ and $s > 1$;*
4. *$\xi_1 = -1$ and $|\xi_2| \neq 1$ if and only if $F(-1) = 0$ and $r \neq 0, 2$;*
5. *ξ_1 and ξ_2 are complex and $|\xi_1| = |\xi_2| = 1$ if and only if $r^2 - 4s < 0$ and $s = 1$.*

Lemma 2. *[39, 40] Let $F(\xi) = \xi^2 + r\xi + s$, is the characteristic equation for equilibrium point $\bar{p}$. Suppose that ξ_1 and ξ_2 are roots of $F(\xi) = 0$. Then, we have:*

1. *If $r^2 > 4s$, then ξ_1; moreover, we have*
   - *(a) $\bar{p}$ is a stable node $\Longleftrightarrow$ $|\xi_1| < 1$ and $|\xi_2| < 1$ if and only if $F(-1) > 0$, $F(1) > 0$;*
   - *(b) $\bar{p}$ is a saddle point $\Longleftrightarrow$ $\xi_1 > 1$ and $|\xi_2| < 1$ (or $|\xi_1| < 1$ and $\xi_2 < -1$) if and only if $F(-1) > 0$, $F(1) < 0$ or $F(-1) < 0$, $F(1) > 0$;*
   - *(c) $\bar{p}$ is an unstable node $\Longleftrightarrow$ $|\xi_1| > 1$ and $|\xi_2| > 1$ if and only if $F(-1) < 0$, $F(1) < 0$.*
2. *If $r^2 < 4s$, then ξ_1 and ξ_2 are complex, and*
   - *(a) $\bar{p}$ is a stable focus if and only if $s < 1$;*
   - *(b) $\bar{p}$ is an unstable focus if and only if $s > 1$.*

Theorem 2. *A topological classification of the equilibrium point P_1 is given as follows:*

(i) *P_1 is stable (sink) if $0 < h < \min\left\{\sqrt[q]{\frac{2\Gamma(1+q)}{ab+ec}}, \sqrt[q]{2(d+e)\Gamma(1+q)}\right\}$;*

(ii) *P_1 is unstable (source) if $h > \max\left\{\sqrt[q]{\frac{2\Gamma(1+q)}{ab+ec}}, \sqrt[q]{2(d+e)\Gamma(1+q)}\right\}$;*

(iii) *P_1 is a saddle if $\sqrt[q]{\frac{2\Gamma(1+q)}{ab+ec}} < h < \sqrt[q]{2(d+e)\Gamma(1+q)}$ or $\sqrt[q]{2(d+e)\Gamma(1+q)} < h < \sqrt[q]{\frac{2\Gamma(1+q)}{ab+ec}}$;*

(iv) *P_1 is non-hyperbolic if $h \in \left\{\sqrt[q]{\frac{2\Gamma(1+q)}{ab+ec}}, \sqrt[q]{2(d+e)\Gamma(1+q)}\right\}$.*

Proof. The Jacobian matrix associated with P_1 is $J(P_1)$. $J(P_1)$ can be written as

$$J(P_1) = \begin{pmatrix} 1 - \frac{h^q}{\Gamma(q+1)}(ab+ec) & 0 \\ \frac{h^q}{(d+e)\Gamma(q+1)} & 1 - \frac{h^q}{(d+e)\Gamma(q+1)} \end{pmatrix},$$

in which case $J(P_1)$ has the eigenvalues $\xi_{11} = 1 - \frac{h^q}{\Gamma(q+1)}(ab+ec)$ and $\xi_{12} = 1 - \frac{h^q}{(d+e)\Gamma(q+1)}$. Applying Theorem 1, one can easily obtain the results (i)–(iv).

Theorem 3. *A topological classification of the equilibrium point P_2 is given as follows.*

(i) *P_2 is unstable (source) if one of the following conditions holds:*

(a) *If $h > \sqrt[q]{\frac{2\Gamma(1+q)}{ab(b-1)}}$ and $b > 1$;*

(b) *if $b < 1$;*

(ii) *P_2 is a saddle if $\sqrt[q]{2d\Gamma(1+q)} < h < \sqrt[q]{\frac{2\Gamma(1+q)}{ab(b-1)}}$ and $b > 1$.*

Proof. The Jacobian matrix associated with P_2 is $J(P_2)$. $J(P_2)$ can be written as

$$J(P_2) = \begin{pmatrix} 1 - \frac{ab(b-1)h^q}{\Gamma(q+1)} & \frac{cbh^q}{\Gamma(q+1)} \\ 0 & 1 + \frac{h^q}{d\Gamma(q+1)} \end{pmatrix},$$

then $J(P_2)$ has the eigenvalues $\xi_{21} = 1 - \frac{ab(b-1)h^q}{\Gamma(q+1)}$ and $\xi_{22} = 1 + \frac{h^q}{d\Gamma(q+1)} > 1$. Applying Theorem 1, one can easily obtain the results (i) and (ii).

Theorem 4. *The equilibrium point P_4 is non-hyperbolic.*

Proof. At $\Delta = 0 \Rightarrow e = \frac{a\left(\left(b+1-\frac{c}{a}\right)^2 - 4b\right)}{4c}$ and by some calculation, the Jacobian matrix associated with P_4 is $J(P_4)$. $J(P_4)$ can be written as

$$J(P_4) = \begin{pmatrix} 1 + \frac{ch^q}{2a\Gamma(q+1)}(a(b+1)-c) & -\frac{ch^q}{2a\Gamma(q+1)}(a(b+1)-c) \\ \frac{4ach^q}{\Gamma(q+1)((b-1)^2a^2+4acd-c^2)} & 1 - \frac{4ach^q}{\Gamma(q+1)((b-1)^2a^2+4acd-c^2)} \end{pmatrix}.$$

Then, the characteristic polynomial of $J(P_4)$ is

$$F_4(\xi) = \xi^2 - \left(2 + \frac{g_3 h^q}{\Gamma(q+1)}\right)\xi + 1 + \frac{g_3 h^q}{\Gamma(q+1)} = 0;$$

where

$$g_4 = \frac{c(a(b+1)-c)}{2a} - \frac{4ac}{(b-1)^2a^2 + 4dac - c^2}.$$

When $J(P_2)$ has the eigenvalues $\xi_{41} = 1$ and $\xi_{42} = 1 + \frac{g_4 h^q}{d\Gamma(q+1)}$, then $|\xi_{41}| = 1$; this completes the proof.

The Jacobian matrix associated with P_6 is $J(P_6)$. $J(P_6)$ can be written as

$$J(P_6) = \begin{pmatrix} 1 - \frac{h^q}{\Gamma(q+1)}\left(3aL_6^2 - (2a(b+1)-c)L_6 + ab + ce\right) & \frac{-cL_6h^q}{\Gamma(q+1)} \\ \frac{h^q}{(d+G_6)\Gamma(q+1)} & 1 - \frac{h^q}{(d+G_6)\Gamma(q+1)} \end{pmatrix}.$$

Then, the characteristic polynomial of $J(P_6)$ is given by

$$F_6(\xi) = \xi^2 + r_6\xi + s_6 = 0; \tag{4.2}$$

where

$$L_6 = \frac{a(1+b-\sqrt{\Delta}) - c}{2a},\ r_6 = -2 + \frac{g_6 h^q}{\Gamma(q+1)},\ \ s_6 = 1 - \frac{g_6 h^q}{\Gamma(q+1)} + k_6\left(\frac{h^q}{\Gamma(q+1)}\right)^2,$$

$$g_6 = 3aL_6^2 - (2a(b+1)-c)L_6 + ab + ce + \frac{1}{d+e+L_6},$$

$$k_6 = \frac{3aL_6^2 - 2a(b+1)L_6 + ab + ce}{d+e+L_6} = \frac{-a\sqrt{\Delta}}{d+e+L_6} < 0.$$

Theorem 5. *A topological classification of the equilibrium point P_6 is given as follows.*

1. *P_6 is an unstable node if and only if $0 < h < \min\left\{\sqrt[q]{\frac{\Gamma(1+q)(g_6-\sqrt{g_6^2-4k_6})}{k_6}}, \sqrt[q]{\frac{\Gamma(1+q)(g_6+\sqrt{g_6^2-4k_6})}{k_6}}\right\}$ and $g_6^2 > 4k_6$.*
2. *If $g_6^2 < 4k_6$, then*
   (a) *P_6 is a stable focus if and only if $h < \sqrt[q]{\frac{g_6\Gamma(1+q)}{k_6}}$;*
   (b) *P_6 is an unstable focus if and only if $h > \sqrt[q]{\frac{g_6\Gamma(1+q)}{k_6}}$.*

Proof. Applying Theorem 2 to (4.2), we have $F(1) = k_6H^2 < 0$ and

1. If $r_6^2 > 4s_6 \Longleftrightarrow g_6^2 > 4k_6$, then P_6 is an unstable node $\Longleftrightarrow |\xi_1| > 1$ and $|\xi_2| > 1$ if and only if $F(-1) = 1 - r_6 + s_6 = k_6H^2 - 2g_6H + 4 < 0$
   $\Longleftrightarrow h > \max\left\{\sqrt[q]{\frac{\Gamma(1+q)(g_6-\sqrt{g_6^2-4k_6})}{k_6}}, \sqrt[q]{\frac{\Gamma(1+q)(g_6+\sqrt{g_6^2-4k_6})}{k_6}}\right\}$;
2. if $r_6^2 < 4s_6 \Longleftrightarrow g_6^2 < 4k_6$, then ξ_1 and ξ_2 are complex, and
   (a) P_6 is a stable focus if and only if $s_6 < 1 \Longleftrightarrow h < \sqrt[q]{\frac{g_6\Gamma(1+q)}{k_6}}$;
   (b) P_6 is an unstable focus if and only if $s_6 > 1 \Longleftrightarrow h > \sqrt[q]{\frac{g_6\Gamma(1+q)}{k_6}}$. □

The Jacobian matrix associated with P_7 is $J(P_7)$. $J(P_7)$ can be written as

$$J(P_7) = \begin{pmatrix} 1 - \frac{h^q}{\Gamma(q+1)}\left(3aL_7^2 - (2a(b+1)-c)L_7 + ab + ce\right) & \frac{-cL_7h^q}{\Gamma(q+1)} \\ \frac{h^q}{(d+G_7)\Gamma(q+1)} & 1 - \frac{h^q}{(d+G_7)\Gamma(q+1)} \end{pmatrix}.$$

The characteristic polynomial of $J(P_7)$ is

$$F_7(\xi) = \xi^2 + r_7\xi + s_7 = 0; \tag{4.3}$$

where

$$L_7 = \frac{a(1+b+\sqrt{\Delta})-c}{2a},\ r_7 = -2 + \frac{g_7h^q}{\Gamma(q+1)},\ \ s_7 = 1 - \frac{g_7h^q}{\Gamma(q+1)} + k_7\left(\frac{h^q}{\Gamma(q+1)}\right)^2,$$
$$g_7 = 3aL_7^2 - (2a(b+1)-c)L_7 + ab + ce + \frac{1}{d+e+L_7},$$
$$k_7 = \frac{3aL_7^2 - 2a(b+1)L_7 + ab + ce}{d+e+L_7} = \frac{a\sqrt{\Delta}}{d+e+L_7} > 0.$$

Theorem 6. *A topological classification of the equilibrium point P_7 is given as follows.*

1. *P_7 is stable (sink) if $h > \max\left\{\sqrt[q]{\frac{\Gamma(1+q)(g_7-\sqrt{g_7^2-4k_7})}{k_7}}, \sqrt[q]{\frac{\Gamma(1+q)(g_7+\sqrt{g_7^2-4k_7})}{k_7}}, \sqrt[q]{\frac{g_7\Gamma(1+q)}{k_7}}\right\}$ and $g_7^2 > 4k_7$;*
2. *P_7 is a saddle if $0 < h < \min\left\{\sqrt[q]{\frac{\Gamma(1+q)(g_7-\sqrt{g_7^2-4k_7})}{k_7}}, \sqrt[q]{\frac{\Gamma(1+q)(g_7+\sqrt{g_7^2-4k_7})}{k_7}}\right\}$;*

3. P_7 *is unstable (source) if* $\max\left\{\sqrt[q]{\frac{\Gamma(1+q)(g_7-\sqrt{g_7^2-4k_7})}{k_7}}, \sqrt[q]{\frac{\Gamma(1+q)(g_7+\sqrt{g_7^2-4k_7})}{k_7}}\right\} < h < \sqrt[q]{\frac{g_7\Gamma(1+q)}{k_7}}$ *and* $g_7^2 > 4k_7$;
4. P_7 *is non-hyperbolic if one of the following cases hold:*
   (a) $h \in \left\{\sqrt[q]{\frac{\Gamma(1+q)(g_7-\sqrt{g_7^2-4k_7})}{k_7}}, \sqrt[q]{\frac{\Gamma(1+q)(g_7+\sqrt{g_7^2-4k_7})}{k_7}}\right\}$ *and* $g_7^2 > 4k_7$;
   (b) $h = \sqrt[q]{\frac{g_7\Gamma(1+q)}{k_7}}$. *and* $g_7^2 < 4k_7$.

Proof. Similarly, by applying Theorem 1 to Eq (4.3), we obtain the results (1)–(4). □

5. Bifurcation

This section rigorously investigates both flip and Neimark-Sacker bifurcations occurring at the equilibrium point P_7 using two distinct methodological approaches.

- The center manifold theorem is utilized to derive the necessary and sufficient conditions for the existence of flip bifurcation.
- The normal form method is applied to characterize the Neimark-Sacker bifurcation structure.

5.1. Flip bifurcation analysis

This section investigates the flip bifurcation occurring at the equilibrium point P_7 as the system parameters (a, b, c, d, e, q, h) vary within a small neighborhood of the bifurcation threshold.

- Let a represent the critical bifurcation parameter.
- Introducing a^* as a small perturbation of a, we derive the following perturbed form of the model in Eq (2.10):

$$\text{Perturbed system} = \text{Original system (2.10)} + O(a^*). \tag{5.1}$$

Now, flip bifurcation occurs at $\xi_{71} = -1$ and other eigenvalue $\xi_{71} \neq -1, 1$ if and only if $F_7(-1) = 0$, $r_7 \neq 0, 2$, i.e.,

$$1 - r_7 + s_7 = 0 \Rightarrow k_7H^2 + 4 = 0 \Rightarrow \frac{H^2(3aL_7^2 - (2(b+1))aL_7 + ab + ce)}{d + e + L_7} + 4 = 0.$$

It follows that

$$a = \frac{H^2ce + 4(L_7 + d + e)}{H^2(2(L_7b + L5) - 3L_7^2 - b)} = b_*(say).$$

Now, let $\mathbb{FB} = \left\{(a, b, c, d, e, q, h) : a = a_*,\ |a + ab - c| < a\sqrt{\Delta}\right\}$. We choose a as a bifurcation parameter and let $u = L - L_7$, $v = G - G_7$ and $r = a - a_*$, where r is a sufficiently small variable. The fixed point P_7 of the map (2.10) is shifted to the origin, and we find that

$$\begin{pmatrix} u_{n+1} \\ v_{n+1} \\ r \end{pmatrix} = \begin{pmatrix} a_{11} & a_{12} & a_{13} \\ a_{21} & a_{22} & 0 \\ 0 & 0 & 1 \end{pmatrix}\begin{pmatrix} u_n \\ v_n \\ r \end{pmatrix} + \begin{pmatrix} f_1(u_n, v_n, r) \\ f_2(u_n, v_n, r) \\ 0 \end{pmatrix}, \tag{5.2}$$

where

$$f_1(u_n, v_n, r) = a_{14}u^2 + a_{15}u_nv_n + a_{16}ru_n + a_{17}ru^2 + a_{18}u^3 + a_{19}ru_n^3,$$
$$f_2(u_n, v_n, r) = a_{24}u^2 + a_{25}u_nv_n + a_{26}u_n^2v_n + a_{27}u_nv_n^2 + a_{28}u^3 + a_{29}v_n^3 + O(|u_n, v_n|^4),$$

and

$$a_{11} = 1 + H(a_*L_7(1 - L_7) + (-a_*L_7 + a_*(1 - L_7))(L_7 - b) - cG_7),\ a_{12} = -HcL_7,$$
$$a_{13} = HL_7(1 - L_7)(L_7 - b), a_{14} = H(-a_*L_7 + a_*(1 - L_7) - a_*(L_7 - b)), a_{15} = -Hc,$$
$$a_{16} = HL_7(1 - L_7) + (-HL_7 + H(1 - L_7))(L_7 - b), a_{17} = -HL_7 + H(1 - L_7) - H(L_7 - b),$$
$$a_{18} = -Ha_*,\ a_{19} = -Hr,\ a_{21} = \frac{HG_7^2}{(e + L_7)^2(d + G_7)},\ a_{22} = 1 - \frac{HG_7}{(d + G_7)^2}\left(1 - \frac{G_7}{e + L_7}\right)$$
$$+ \frac{1}{d + G_7}\left(\frac{-HG_7}{e + L_7} + H\left(1 - \frac{G_7}{e + L_7}\right)\right),\ a_{23} = 0,\ a_{24} = \frac{-HG_7^2}{(e + L_7)^3(d + G_7)},$$
$$a_{25} = \frac{-HG_7^2}{(e + L_7)^2(d + G_7)^2} + \frac{2HG_7}{(e + L_7)^2(d + G_7)},\ a_{26} = \frac{HG_7^2}{(e + L_7)^3(d + G_7)^2} - \frac{2HG_7}{(e + L_7)^3(d + G_7)},$$
$$a_{27} = \frac{HG_7^2}{(e + L_7)^2(d + G_7)^3} - \frac{2HG_7}{(e + L_7)^2(d + G_7)^2} + \frac{H}{(e + L_7)^2(d + G_7)},\ a_{28} = \frac{HG_7^2}{(e + L_7)^4(d + G_7)},$$
$$a_{29} = \frac{-HG_7}{(d + G_7)^4}\left(1 - \frac{G_7}{e + L_7}\right) + \frac{1}{(d + G_7)^3}\left(\frac{-HG_7}{e + L_7} + H\left(1 - \frac{G_7}{e + L_7}\right)\right) + \frac{H}{(e + L_7)(d + G_7)^2}.$$

The linearization of the map (5.2) at $(0, 0, 0)$ gives:

$$J = \begin{pmatrix} a_{11} & a_{12} & a_{13} \\ a_{21} & a_{22} & 0 \\ 0 & 0 & 1 \end{pmatrix}.$$

We will construct an invertible matrix T

$$T = \begin{pmatrix} a_{11} & a_{12} & 0 \\ -1 - a_{11} & \xi_{71} - a_{11} & \frac{L_7(L_7-1)}{a_{12}} \\ 0 & 0 & 1 \end{pmatrix}$$

and

$$\begin{pmatrix} u_n \\ v_n \\ r \end{pmatrix} = T \begin{pmatrix} X_n \\ Y_n \\ r \end{pmatrix}.$$

The map (5.2) yields

$$\begin{pmatrix} X_{n+1} \\ Y_{n+1} \\ r \end{pmatrix} = \begin{pmatrix} -1 & 0 & 0 \\ 0 & \xi_{72} & 0 \\ 0 & 0 & 1 \end{pmatrix} \begin{pmatrix} X_n \\ Y_n \\ r \end{pmatrix} + \begin{pmatrix} F_1(X_n, Y_n, r) \\ F_2(X_n, Y_n, r) \\ 0 \end{pmatrix}. \tag{5.3}$$

Here

$$F_1(X_n, Y_n, r) = rK_{11}(X_n + Y_n) + K_{12}X_nY_n + K_{13}X_n^2 + K_{14}Y_n^2 + O(|X, Y|)^3,$$
$$F_2(X_n, Y_n, r) = rK_{21}(X_n + Y_n) + K_{22}X_nY_n + K_{23}X_n^2 + K_{24}Y_n^2 + O(|X, Y|)^3,$$

and

$$
\begin{aligned}
K_{11} &= \frac{a_{15}(\xi_{72}-a_{11})-a_{12}a_{24}}{\xi_{72}+1}L_7(L_7-1)+\frac{a_{16}(\xi_{72}-a_{11})}{\xi_{72}+1},\\
K_{12} &= 2a_{12}\left(\frac{a_{14}(\xi_{72}-a_{11})-a_{12}a_{23}}{\xi_{72}+1}\right)+\frac{a_{15}(\xi_{72}-a_{11})-a_{12}a_{24}}{\xi_{72}+1}(\xi_{72}-2a_{11}-1),\\
K_{13} &= a_{12}\left(\frac{a_{14}(\xi_{72}-a_{11})-a_{12}a_{23}}{\xi_{72}+1}\right)-\frac{a_{15}(\xi_{72}-a_{11})-a_{12}a_{24}}{\xi_{72}+1}(a_{11}+1),\\
K_{14} &= a_{12}\left(\frac{a_{14}(\xi_{72}-a_{11})+a_{12}a_{23}}{\xi_{72}+1}\right)+\frac{a_{15}(\xi_{72}-a_{11})-a_{12}a_{24}}{\xi_{72}+1}(\xi_{72}-a_{11}),\\
K_{21} &= \left(\frac{a_{15}(1+a_{11})+a_{12}a_{24}}{\xi_{72}+1}\right)L_7(L_7-1)+\frac{a_{16}(1+a_{11})}{\xi_{72}+1}a_{12},\\
K_{22} &= 2a_{12}\left(\frac{a_{14}(1+a_{11})+a_{12}a_{23}}{\xi_{72}+1}\right)+\frac{a_{15}(1+a_{11})+a_{12}a_{24}}{\xi_{72}+1}(\xi_{72}-2a_{11}-1),\\
K_{23} &= a_{12}\left(\frac{a_{14}(1+a_{11})+a_{12}a_{23}}{\xi_{72}+1}\right)-\frac{a_{15}(1+a_{11})+a_{12}a_{24}}{\xi_{72}+1}(a_{11}+1),\\
K_{24} &= a_{12}\left(\frac{a_{14}(1+a_{11})+a_{12}a_{23}}{\xi_{72}+1}\right)+\frac{a_{15}(1+a_{11})+a_{12}a_{24}}{\xi_{72}+1}(\xi_{72}-a_{11}).
\end{aligned}
$$

If we apply the center manifold theory, the local stability of the equilibrium $(X, Y) = (0, 0)$ near the critical parameter value $r = 0$ is determined by a one-parameter family of reduced equations restricted to the center manifold, given by

$$W^c(0,0,0) = \{(X_n, Y_n, r) \in \mathbb{R} : Y_n = h(0,0) = 0,\ Dh(0,0) = 0\},$$

for X_n and a small r. Let

$$h(X_n, r) = h_1 r^2 + h_2 X_n r + h_3 X^2 + O(|X_n, r|^3). \tag{5.4}$$

Then $h(X_n, r)$ must satisfy

$$N(h(X_n, r)) = h(-X_n + F_1(X_n, h(X_n, r), r), r) - \xi_{72} h(X_n, r) - F_2(X_n, h(X_n, r), r) = 0. \tag{5.5}$$

From (5.4) and (5.5), we get

$$h_1 = 0,\ h_2 = \frac{K_{24}}{\xi_{72}+1},\ h_3 = \frac{K_{21}}{\xi_{72}-1}.$$

The map is transformed as follows:

$$F : X_n \to -X_n + K_{11}X^2 + K_{14} r X_n + O(|X_n, Y_n|^3). \tag{5.6}$$

It follows that

$$
\begin{aligned}
\Phi_1 &= \left(2\frac{\partial^2 F}{\partial X_n \partial r} + \frac{\partial F}{\partial r}\frac{\partial^2 F}{\partial X_n^2}\right)\Bigg|_{(0,0)} = 2(K_{14} - K_{11}) \neq 0,\\
\Phi_2 &= \left(\frac{1}{3}\frac{\partial^3 f}{\partial X_n^3} + \frac{1}{2}\left(\frac{\partial^2 f}{\partial X_n^2}\right)^2\right)\Bigg|_{(0,0)} = 2K_{11}^2 \neq 0.
\end{aligned}
$$

Therefore, flip bifurcation occurs in the map (2.10) at P_7 for $a = a_*$.

Theorem 7. *If $\Phi_2 \neq 0$, then the system* (2.10) *undergoes a flip bifurcation at P_7 when the parameter a varies in a small neighborhood of a_*. Moreover, if $\Phi_2 > 0$ (respectively, $\Phi_2 < 0$), then the period-two orbit bifurcated from the fixed point is stable (respectively, unstable). Hence, the occurrence of a flip bifurcation shows that the prey and predator populations may coexist in a 2-periodic orbit under certain conditions.*

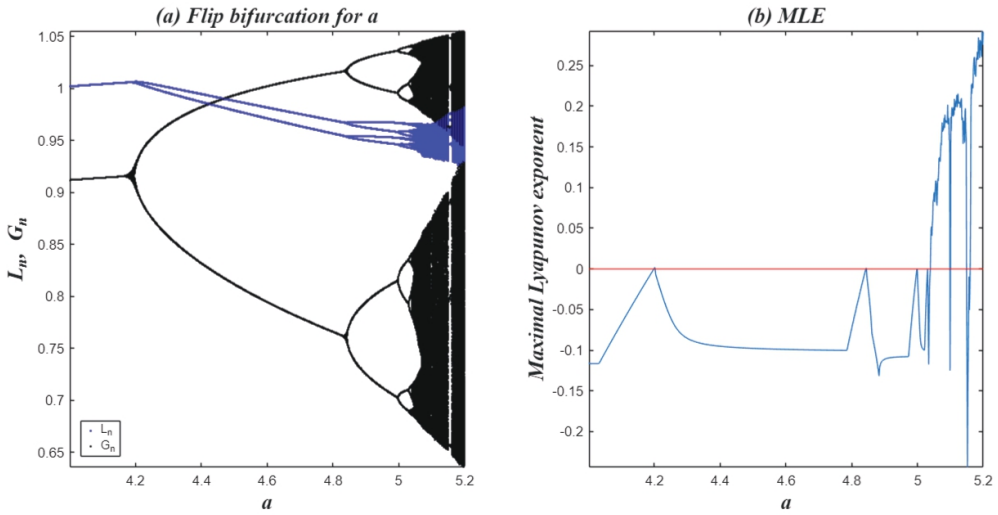

Figure 1. (a) Flip bifurcation of (2.10) with respect to a. (b) The corresponding Maximal Lyapunov exponent.

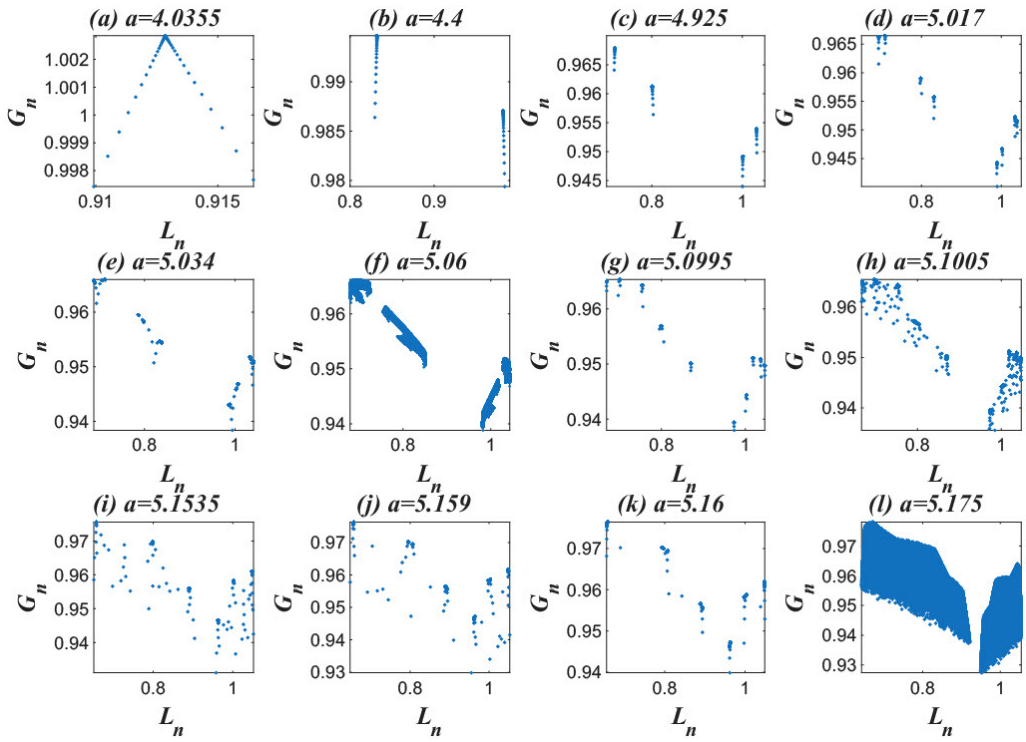

Figure 2. Phase portraits of the system (2.10) with respect to Figure 1 for $a = 4.035 : 5.175$.

5.2. Neimark-Sacker bifurcation

This subsection presents a bifurcation analysis of the discrete fractional-order predator-prey system (2.10), focusing on the Neimark-Sacker bifurcation for parameter values belonging to the following set:

$$\mathbb{NB} = \left\{(a,b,c,d,e,q,h) : h = \sqrt[q]{\frac{g_7\Gamma(1+q)}{k_7}} = h_{ns},\ g_7^2 < 4k_7\right\}.$$

Let h^s be the perturbation of h_* where $|h_*| \ll 1$. Therefore, the model perturbation is

$$\begin{aligned} L_{n+1} &= L_n + \frac{(h+h_*)^q}{\Gamma(q+1)}\left[aL_n(1-L_n)(L_n-b) - cL_nG_n\right] = f(L_n,G_n,h_*),\\ G_{n+1} &= G_n + \frac{(h+h_*)^q}{\Gamma(q+1)}\left[\frac{G_n}{d+G_n}\left(1-\frac{G_n}{e+L_n}\right)\right] = g(L_n,G_n,h_*). \end{aligned} \tag{5.7}$$

If $u_n = L_n - L_7,\ v_n = G_n - G_7$, then equilibrium point P_7 becomes the origin. By using Taylor series at $(u_n, v_n) = (0,0)$ expanding f and g to the third order, the model (5.7) becomes

$$\begin{aligned} u_{n+1} &= k_{10}u_n + k_{01}v_n + k_{20}u^2 + k_{11}u_nv_n + k_{02}v_n^2 + k_{30}u_n^3 + k_{21}u_n^2v_n + k_{12}u_nv_n^2 + k_{03}v_n^3 + O((|u_n| + |v_n|)^4),\\ v_{n+1} &= p_{10}u_n + p_{01}v_n + p_{20}u^2 + p_{11}u_nv_n + p_{02}v_n^2 + p_{30}u_n^3 + p_{21}u_n^2v_n + p_{12}u_nv_n^2 + p_{03}v_n^3 + O((|u_n| + |v_n|)^4), \end{aligned} \tag{5.8}$$

where

$$\begin{aligned} &k_{10} = 1 + \frac{(h+h_*)^q((-3L_7^2 + (2b+2)L_7 - b)a - cG_7)}{\Gamma(1+q)},\ k_{01} = \frac{-(h+h_*)^q cL_7}{\Gamma(1+q)}, k_{20} = \frac{(h+h_*)^q a(-3L_7+1+b)}{\Gamma(1+q)},\\ &k_{11} = \frac{-(h+h_*)^q}{\Gamma(1+q)}, k_{02} = 0, k_{30} = \frac{-(h+h_*)^q a}{\Gamma(1+q)},\ k_{21} = 0,\ k_{12} = 0,\ k_{03} = 0,\ p_{10} = \frac{(h+h_*)^q G_7^2}{(e+L_7)^2\Gamma(1+q)(d+G_7)},\\ &p_{01} = \frac{((e+L_7-2G_7)d - G_7^2)(h+h_*)^q + (e+L_7)\Gamma(1+q)(d+G_7)^2}{(e+L_7)\Gamma(1+q)(d+G_7)^2},\ p_{20} = \frac{-(h+h_*)^q G_7^2}{(e+L_7)^3\Gamma(1+q)(d+G_7)},\\ &p_{11} = \frac{(h+h_*)^q G_7(G_7+2d)}{(e+L_7)^2\Gamma(1+q)(d+G_7)^2},\ p_{02} = \frac{-(h+h_*)^q d(L_7+d+e)}{(e+L_7)\Gamma(1+q)(d+G_7)^3},\ p_{30} = \frac{(h+h_*)^q d(L_7+d+e)}{(e+L_7)\Gamma(1+q)(d+G_7)^4},\\ &p_{21} = \frac{-(h+h_*)^q G_7(G_7+2d)}{(e+L_7)^3\Gamma(1+q)(d+G_7)^2}, p_{12} = \frac{(h+h_*)^q d^2}{(e+L_7)^2\Gamma(1+q)(d+G_7)^3},\ p_{03} = \frac{(h+h_*)^q d(L_7+d+e)}{(e+L_7)\Gamma(1+q)(d+G_7)^4}. \end{aligned}$$

The characteristic equation of the model (5.8) is

$$\xi^2 + r_n(h_*)\xi + s_n(h_*) = 0, \tag{5.9}$$

where

$$\begin{aligned} r_n(h_*) &= -2 + \frac{(h+h_*)^q}{\Gamma(1+q)}\tau,\ s_n(h_*) = 1 - \frac{(h+h_*)^q}{\Gamma(1+q)}\tau + \left(\frac{(h+h_*)^q}{\Gamma(1+q)}\right)^2\delta,\\ \tau &= (3L_7^2 - 2L_7b - 2L_7 + b)a - cG_7 - \frac{(e-2G_7+L_7)d - G_7^2}{(e+L_7)(d+G_7)^2},\\ \delta &= \frac{1}{(e+L_7)^2(d+G_7)^2}\left(-3L_7^4ad + \left(\left(2\left(b-3e+3G_7+1\right)\right)d + 3G_7^2\right)aL_7^3 + ((((6e-4b-4)G_7\right.\\ &\quad \left.-3e^2 + (4b+4)e - b\right)d - \left(2b-3e+2\right)G_7^2\Big)a - cdG_7\Big)L_7^2 + ((((2b-4(b+1)e)G_7 + 2e((1+b)e-b))d\\ &\quad - ((2(1+b))e-b)G_7^2\Big)a - \Big(((2e-3G_7))d - 2G_7^2\Big)cG_7\Big)L_7 - e\left((e-2G_7)d - G_7^2\right)(G_7c+ab)\Big). \end{aligned}$$

The roots of (5.9) are

$$\xi_{1,2}(h_*) = \frac{1}{2}\left(-r_n(h_*) \pm i\sqrt{4s_n(h_*) - r_n^2(h_*)}\right). \tag{5.10}$$

For $4s_n(h_*) - r_n^2(h_*) > 0$ always. From $|\xi_{1,2}(h_*)| = 1$ and $h_* = 0$, we have $|\xi_{1,2}(h_*)| = \sqrt{s_n(h_*)}$ and

$$l = \left.\frac{d\left|\xi_{1,2}(h_*)\right|}{dh_*}\right|_{h_*=0} = \frac{-qh^{q-1}(\Gamma(1+q)\tau - 2h^q\delta)}{2\Gamma(1+q)^2\sqrt{s_n(0)}} \neq 0.$$

Additionally, it is necessary that when $h_* = 0$, $\xi_{1,2}^i \neq 1$, $i = 1, 2, 3, 4$, which is equivalent to $r_n(0) \neq \pm 2, 0, 1$. For a study of the normal form, let $I_n = Im(\xi_{1,2})$ and $R_n = Re(\xi_{1,2})$. We define $T_n = \begin{pmatrix} 0 & 1 \\ I_n & R_n \end{pmatrix}$. With the transformation $T_n = \begin{pmatrix} u_n \\ v_n \end{pmatrix} = T_n \begin{pmatrix} \bar{x}_n \\ \bar{y}_n \end{pmatrix}$, the model (5.8) becomes

$$\begin{aligned} \bar{x}_{n+1} &= R_n\bar{x}_n - I_n\bar{y}_n + f_{11}(\bar{x}_n, \bar{y}_n), \\ \bar{y}_{n+1} &= I_n\bar{x}_n + R_n\bar{y}_n + g_{11}(\bar{x}_n, \bar{y}_n), \end{aligned} \tag{5.11}$$

where the variables $(\bar{x}_n, \bar{y}_n)$ have an order of at least two denote the terms in the model (5.11) with the functions f_{11} and g_{11}, respectively.

The following discriminatory amount Φ_n must be nonzero in order to undergo Neimark-Sacker bifurcation:

$$\Phi_n = -Re\left[\frac{(1-2\bar{\xi})\bar{\xi}^2}{1-\xi}\lambda_{11}\lambda_{20}\right] - \frac{1}{2}|\lambda_{11}|^2 - |\lambda_{02}|^2 + Re(\bar{\xi}\lambda_{21}),$$

where

$$\begin{aligned} \lambda_{20} &= \frac{R_n}{8}(2p_{02} - R_nk_{02} - k_{11} + 4I_nk_{02} + i(4I_nk_{02} - 2k_{02} - 2R_nk_{02})) + \frac{I_n}{4}k_{11} + \frac{p_{11}}{8} \\ &\quad + \frac{R_nk_{20} - 2p_{20} + R_n^3k_{02} - R_n^2p_{02} - R_n^2k_{11} + R_np_{11}}{4I_n} + \frac{i}{8}(4I_np_{02} + 2I_n^2k_{02} - 2k_{20}), \\ \lambda_{11} &= \frac{I_n}{2}(p_{02} - R_nk_{02}) + \frac{i}{2}(I_n^2k_{02} + k_{20} + R_nk_{11} + R_n^2k_{02}) \\ &\quad + \frac{p_{20} - R_nk_{20} + R_np_{11} - R_n^2k_{11} - 2R_n^2p_{02} + 2R_n^3k_{02}^2I_n}{2I_n}, \\ \lambda_{02} &= \frac{1}{4}I_n(2R_nk_{02} + k_{11} + p_{02}) + \frac{i}{4}(p_{11} + 2R_np_{02} - 2R_nk_{11} - k_{20}) \\ &\quad - \frac{p_{20} - R_nk_{20} + R_np_{11} - R_n^2k_{11} + R_n^2p_{02} - R_n^3k_{02}4I_n}{4I_n} + \frac{1}{4}k_{02}i(I_n^2 - 3R_n^2), \\ \lambda_{21} &= \frac{3p_{03}}{8}(I_n^2 + R_n^2) + \frac{p_{21}}{8} + \frac{R_n}{4}(k_{21} + p_{12}) + k_{12}(\frac{I_n2 + 3R_n^2 - 2R_n}{8}) + \frac{3}{8}k_{30} + i\frac{3}{8}k_{03}(I_n^2 + 2R_n^2) \\ &\quad + i\frac{3I_nR_n}{8}k_{12} - \frac{p_{12}I_n}{8}i - i\frac{3I_nR_n}{8}p_{03} - \frac{i}{8I_n}(p_{20}1 - R_nk_{30} + R_np_{21} - R_n^2k_{21} + R_n^2p_{12} \\ &\quad - R_n^3k_{12} + R_n + p_{03} - R_n^4k_{03}). \end{aligned}$$

Based on the preceding analysis, the following theorem characterizes the direction and stability of the Neimark-Sacker bifurcation.

Theorem 8. *(Neimark-Sacker bifurcation) Assume* $\Phi_n \neq 0$. *Then the system* (2.10) *undergoes a Neimark-Sacker bifurcation at the equilibrium point* P_7 *when* h *crosses* h_*. *Furthermore,*

- *if* $\Phi_n < 0$, *a* ***stable*** *invariant circle appears via a subcritical bifurcation;*
- *if* $\Phi_n > 0$, *an* ***unstable*** *invariant circle appears via a supercritical bifurcation.*

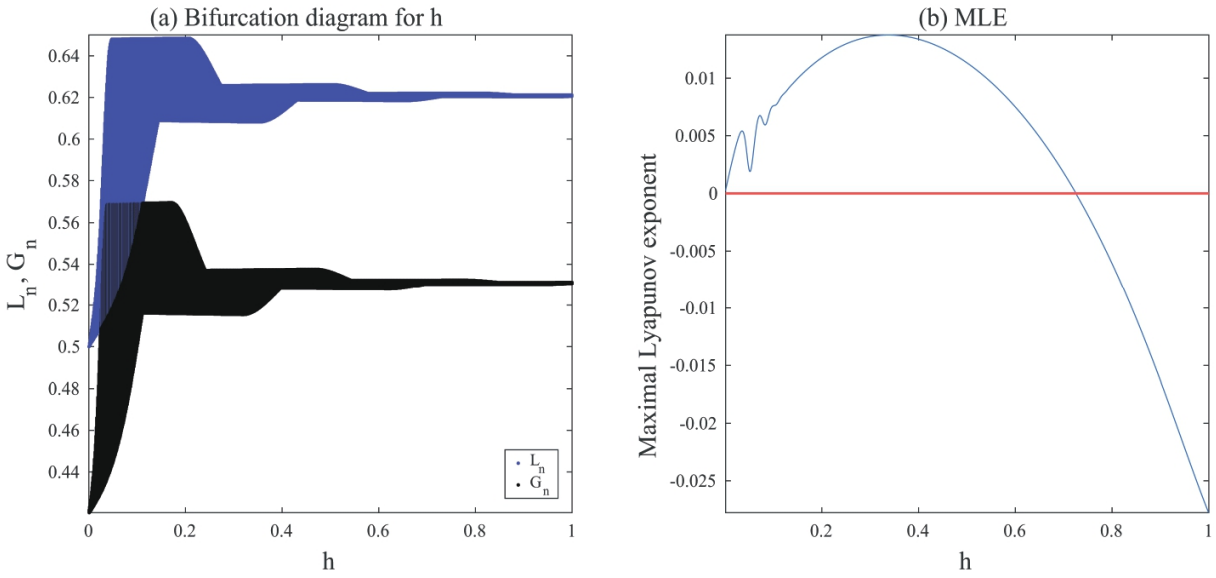

Figure 3. (a) Flip bifurcation of the system (2.10) for a. (b) The corresponding Maximal Lyapunov exponent.

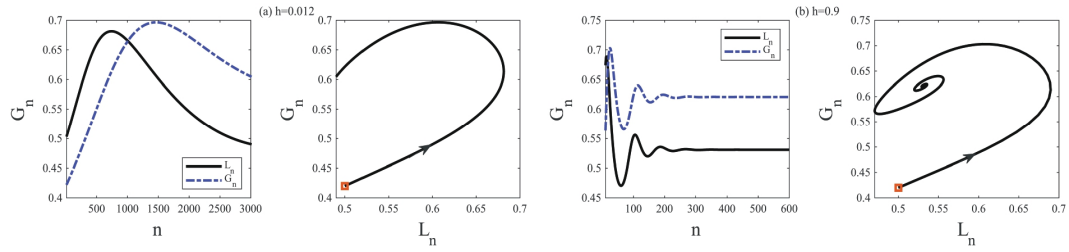

Figure 4. Phase portraits of the system (2.10) with respect to Figure 3 at $h = 0.012, 0.9$.

Chaotic behavior in population dynamics offers a more accurate representation of natural variations than straightforward periodic cycles. This complexity has two effects on the stability of ecosystems. While chaotic lows can make populations more vulnerable and raise the risk of extinction, chaos can also help biodiversity by making things less stable. It does this by using temporal niche partitioning to stop competitive exclusion, which lets different species live together by using different parts of the chaotic oscillations.

The analysis of bifurcations not only clarifies population-level impacts but also functions as a practical tool for ecosystem management. Bifurcations do not simply happen in concepts; they are the points at which a stable system can transform into a different state, which could be one that has fallen apart. When a system gets close to these crucial points, it starts to give out early warning signs, including taking longer to fix problems. Managers can learn about risky parameter ranges ahead of

time by locating these thresholds and looking for signs that they are likely to happen. This foresight makes it possible to take steps to protect the system and stop a rapid, possibly irreversible, collapse by lowering the amount of nutrients that get into a lake or restricting the amount of harvest pressure.

6. Numerical simulation

In this section, we numerically examine the behavior of model (2.10) using the analysis from the previous sections. Due to the lack of exact analytic solutions for most fractional-order differential equations, we use approximation and numerical techniques. For all figures, the fixed parameters are $(b, c, d, e, q) = (0.2, 0.25, 7.5, 0.09, 0.95)$ and the initial condition is $(L_1, G_1) = (0.6, 0.5)$. The remaining parameters are listed in Table 1.

Table 1. Parameters of the figures.

Figure	a	h
1,2	4 : 5.2	0.8
3	1	0 : 1
4(a),(b)	1	0.012, 0.9
5(a)	5.175	0.8
5(b)–(e)	5.175	0.8
6(a)	5.175	0.8
6(a)–(e)	5.175	0.8
7(a)	5.175	0.8
7(a)–(e)	5.175	0.8

Figure 1 presents the bifurcation diagram for the system (2.10) with respect to parameter a, using the specified parameter set above. The system undergoes a flip bifurcation followed by chaotic dynamics via a period-doubling cascade. Specifically, for $a \in (5.04, 5.2)$, the system exhibits (i) a sequence of period-doubling bifurcations leading to chaos, and (ii) an intermittent quasi-periodic window within the sub-interval $(5.149, 5.163)$. The bifurcation diagrams are shown in Figure 1, and the corresponding maximal Lyapunov exponent (MLE) spectrum is displayed. Chaotic behavior is indicated by systems with positive MLE values. It is clear from the bifurcation diagrams that a period-doubling bifurcation begins at $a \approx 4.25$, when the interior equilibrium point becomes unstable.

Using the same parameter configuration as in Figures 1 and 2 depicts the dynamic behavior of the system (2.10). Under these conditions, Figure 2 illustrates a stable equilibrium state. The bifurcation sequence evident in Figure 2 exhibits periodic orbits of periods 2, 4, 8, and 16. Numerical simulations further confirm that variation of the parameter a induces: (i) The gradual disappearance of 2^n-periodic orbits, and (ii) the enlargement of chaotic attractors—observations that are in excellent agreement with our theoretical findings. In Figure 3, the orbit diagram of the prey and predator populations, and MLEs are shown together with other fixed parameter values in Table 1 and where $h \in (0, 1)$. We establish a fixed point $P_7 = (0.5309, 0.6209)$ and assess the bifurcation point for the system (2.10) at $h_* = 0.724$. The eigenvalues are $\xi_{71}, \xi_{72} = 0.9794559160 \pm 0.06752477036i$. This figure shows transition of trajectory from a fixed point to Niemark-Sacker bifurcation and finally to a chaotic attractor. The phase portrait of Figure 3 is shown in Figure 4.

From an ecological perspective, the emergence of chaos signifies that minor alterations in the environment or slight modifications in parameters can precipitate substantial, unpredictable fluctuations in population densities. This degree of sensitivity may manifest in erratic population cycles, abrupt declines, or rapid surges. Conversely, stabilization within specific parameter regimes indicates that predator-prey dynamics or stable coexistence will revert to equilibrium. These conditions are typically associated with enhanced ecological resilience. It is important to emphasize that this behavior occurs inside the discrete-time framework established by the Euler scheme. While this discrete form is frequently utilized to examine the population dynamics of seasonally breeding species, it may not be dynamically equal to its continuous-time equivalent. Similar dynamic phenomena have been observed in different discretized ecological systems, indicating that the underlying mechanisms are not merely numerical artifacts, despite the quantitative thresholds varying according to the individual discretization approach utilized.

7. Chaos control

Managing chaos and bifurcations is vital in population models, particularly those related to the biological reproduction of species. Discrete-time models often display more intricate dynamics than their continuous counterparts. To avoid unpredictable outcomes in populations, it is critical to apply chaos control methods. In all numerical simulations for the three types of chaos control discussed below, we will use the same parameters as in Figure 3 with $a = 4.4$ (where chaos occurs).

7.1. Pole placement technique

In this subsection, we examine two feedback control strategies aimed at steering unstable trajectories toward stable ones. We begin by applying the Ott-Grebogi-Yorke (OGY) control method to the system (2.10), a strategy developed by Ott et al. [41], using the parameter a as a control parameter. We express the system (2.10) as follows:

$$\begin{aligned} L_{n+1} &= L_n + H\left[aL_n\left(1 - L_n\right)\left(L_n - b\right) - cL_nG_n\right] = X(L_n, G_n, a), \\ G_{n+1} &= G_n + H\left[\frac{G_n}{d + G_n}\left(1 - \frac{G_n}{e + L_n}\right)\right] = Y(L_n, G_n, a). \end{aligned} \tag{7.1}$$

where $H = \frac{h^q}{\Gamma(q+1)}$. Here, a is chosen as the control parameter, allowing chaos control to be achieved through minimal perturbations. To implement this, we constrain a to a small interval $a \in (a_0 - \epsilon, a_0 + \epsilon)$, where $\epsilon > 0$ and a_0 represents the nominal value within the chaotic region. By applying a stabilizing feedback control strategy, the trajectory is guided toward the desired orbit. Let $P_7 = (L_7, e + L_7)$ be an unstable equilibrium point of the system (2.10) in the chaotic region, resulting from period-doubling bifurcation or Neimark-Sacker bifurcation. In the vicinity of this unstable equilibrium point $P_7 = (L_7, e + L_7)$, the system (7.1) can be approximated by the following linear map:

$$\begin{bmatrix} L_{n+1} - L_7 \\ G_{n+1} - G_7 \end{bmatrix} \approx J\left(L_7, G_7, a_0\right) \begin{bmatrix} L_n - L_7 \\ G_n - G_7 \end{bmatrix} + N\left[a - a_0\right], \tag{7.2}$$

where

$$J(L_7, G_7, a_0) = \begin{bmatrix} X_L|_{(L_7,G_7,a_0)} & X_G|_{(L_7,G_7,a_0)} \\ Y_L|_{(L_7,G_7,a_0)} & Y_G|_{(L_7,G_7,a_0)} \end{bmatrix} = \begin{bmatrix} 1 - H\left(3a_0L_7^2 - (2a_0(b+1) - c)L_7 + a_0b + ce\right) & -cL_7H \\ \frac{H}{d+e+L_7} & 1 - \frac{H}{d+e+L_7} \end{bmatrix},$$

and

$$N = \begin{bmatrix} \frac{\partial X(L_7,G_7,a_0)}{\partial a} \\ \frac{\partial Y(L_7,G_7,a_0)}{\partial a} \end{bmatrix} = \begin{bmatrix} H(1-L_7)(L_7-b) \\ 0 \end{bmatrix}.$$

Additionally, the system (7.1) is controllable if the following matrix condition is satisfied:

$$C = [N{:}JN] = \begin{bmatrix} H(1-L_7)(L_7-b) & \left(1 - \frac{h^q}{\Gamma(q+1)}\left(3a_0L_7^2 - (2a_0(b+1) - c)L_7 + a_0b + ce\right)\right)H(1-L_7)(L_7-b) \\ 0 & \frac{H^2L_7(1-L_7)(L-b)}{d+e+L_7} \end{bmatrix},$$

and it is of rank 2. Moreover, taking $[a - a_0] = -J\begin{bmatrix} L_n - L_7 \\ G_n - G_7 \end{bmatrix}$, where $Q = \begin{bmatrix} \nu_1 & \nu_2 \end{bmatrix}$, then the system (7.2) can be written as

$$\begin{bmatrix} L_{n+1} - L_7 \\ G_{n+1} - G_7 \end{bmatrix} \approx [J - NQ]\begin{bmatrix} L_n - L_7 \\ G_n - G_7 \end{bmatrix}. \tag{7.3}$$

Moreover, the controlled version of the system (2.10) is expressed as:

$$\begin{aligned} L_{n+1} &= L_n + \frac{h^q}{\Gamma(q+1)}\left[(a_0 - \nu_1(L_n - L_7) - \nu_2(G_n - G_7))L_n(1 - L_n)(L_n - b) - cL_nG_n\right], \\ G_{n+1} &= G_n + \frac{h^q}{\Gamma(q+1)}\left[\frac{G_n}{d + G_n}\left(1 - \frac{G_n}{e + L_n}\right)\right]. \end{aligned} \tag{7.4}$$

Moreover, the equilibrium point P_7 is considered to be locally asymptotically stable if and only if the eigenvalues of the matrix $[J - NQ]$ are located within the open unit disk. The Jacobian matrix $[J - NQ]$ for the controlled system (7.4) is expressed as follows:

$$J - NQ = \begin{bmatrix} 1 - HJ_1 & \left(-(L_7^2 - 1)(L_7 - b)\nu_2 + cL\right)H \\ \frac{H}{d+e+L_7} & 1 - \frac{H}{d+e+L_7} \end{bmatrix},$$

where $J_1 = \left((b\nu_1 + 3a_0)L_7^2 - \nu_1L_7^3 + (\nu_1 + (-2b-2)a_0 + c)L_7 + ba_0 - b\nu_1 + ce\right)$. The characteristic equation for the Jacobian matrix $[J - NQ]$ is provided by

$$\mathbb{P}_p(\xi) = \xi^2 - Tr_p\xi + Det_p = 0, \tag{7.5}$$

where

$$\begin{aligned} &Tr_p = \xi_{p1} + \xi_{p2} = 2 - \mu_1H,\ Det_p = \xi_{p1}\xi_{p2} = 1 - \mu_1H + \mu_2H^2, \\ &\mu_1 = (3a - \nu_1)L_7^2 - (2ab + 2a - c - (1+b)\nu_1)L_7 + ab - b\nu_1 + ce + \frac{1}{d+e+L_7}, \\ &\mu_2 = \frac{1}{d+e+L_7}\left((\nu_1 + \nu_2 - 3a)L_7^2 + ((2a - \nu_1 - \nu_2)b + 2a - 2c - \nu_1 - \nu_2)L_7 + (\nu_1 + \nu_2 - a)b - ce\right). \end{aligned} \tag{7.6}$$

The equilibrium point P_7 of system (7.1) is locally asymptotically stable if and only if the eigenvalues ξ_i of the matrix $J - NQ$ satisfy

$$|\xi_i| < 1 \quad \text{for} \quad i = 1, 2.$$

The methodology for positioning these eigenvalues at the desired locations within the unit circle is termed the pole-placement technique, with the corresponding eigenvalues designated as regulating poles.

Remark 1. *The stability condition* (7.3) *implies that*

- *The system's dynamics are governed by the spectral radius* $\rho(J - NQ) < 1$.
- *Proper selection of V ensures all regulating poles lie in the stable region.*
- *This technique provides systematic control over the system's transient response.*

For the controllability matrix J, we take a transformation

$$T = WM,$$

where

$$M = \begin{bmatrix} r_7 & 1 \\ 1 & 0 \end{bmatrix}.$$

The characteristic equation,

$$|\xi I - J_7| = \xi^2 - r_7\xi + s_7 = 0$$

gives r_7 in (4.2). The system (7.5) gives the characteristic equation

$$|\xi I - J_7 + NQ| = \xi^2 - r_p\xi + s_p = 0,$$

where

$$\begin{aligned}
r_p &= \xi_{p1} + \xi_{p2} = 2 - \mu_1 H, \\
s_p &= \xi_{p1}\xi_{p2} = 1 - \mu_1 H + \mu_2 H^2, \\
\mu_1 &= (3a - \nu_1)L_7^2 - (2ab + 2a - c - (1 + b)\nu_1)L_7 + ab - b\nu_1 + ce + \frac{1}{d + e + L_7}, \\
\mu_2 &= \frac{1}{d + e + L_7}\Big((\nu_1 + \nu_2 - 3a)L_7^2 + ((2a - \nu_1 - \nu_2)b + 2a - 2c - \nu_1 - \nu_2)L_7 + (\nu_1 + \nu_2 - a)b - ce\Big).
\end{aligned} \tag{7.7}$$

From [42], the gain matrix V can be determined as

$$V = \Big[s_p - s_7, r_p - r_7\Big]T^{-1}.$$

Thus the system (7.1) is completely controlled if we can get a gain matrix V by the pole-placement method.

For $\nu_1 = 0.2$ and $\nu_2 \in (-2.45, 3)$, the system (7.4) is stable at the fixed point P_7. Figure 5(a) depicts a bifurcation diagram which shows a periodic solution in the system. If we compare it with Figure 5(b)–(e), it is easily seen that the chaos has been reduced to the periodic windows.

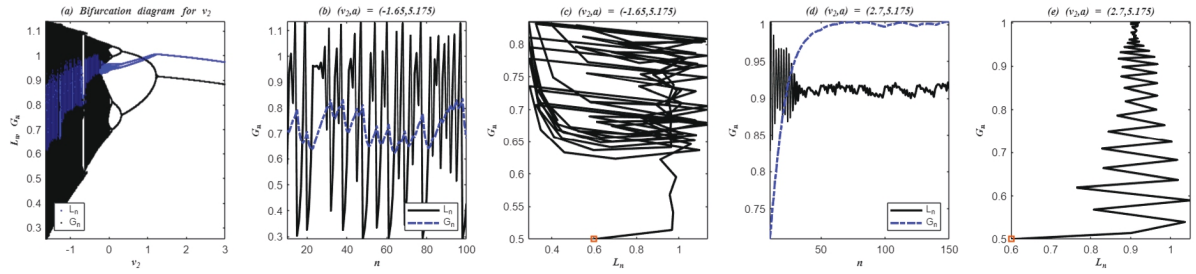

Figure 5. (a) Bifurcation for the OGY parameter ν_2. (b)–(e) Phase portraits of the system (7.4) inside and outside stability interval for ν_2 and the red circle refers to the initial condition.

If we take parameters of system (7.4) as shown in Table 1, Eq (7.5) becomes

$$\xi^2-(0.7469653217+0.04078341845\nu_1)\xi-1.471603606-0.03683270510\nu_1+0.003950713345\nu_2=0. \tag{7.8}$$

7.2. *Hybrid control method*

Additionally, The authors of [43] utilized the same technique to control the chaos resulting from Neimark-Sacker bifurcations. If the system (2.10) experiences bifurcation at P_7, the associated controlled system is represented as follows:

$$\begin{aligned} L_{n+1} &= \nu\left(L_n+\frac{h^q}{\Gamma(q+1)}\left[aL_n(1-L_n)(L_n-b)-cL_nG_n\right]\right)+(1-\nu)L_n,\\ G_{n+1} &= \nu\left(G_n+\frac{h^q}{\Gamma(q+1)}\left[\frac{G_n}{d+G_n}\left(1-\frac{G_n}{e+L_n}\right)\right]\right)+(1-\nu)G_n, \end{aligned} \tag{7.9}$$

where $0<\nu<1$. The control strategy outlined in (7.9) integrates both parameter perturbation and feedback control. By carefully choosing the control parameter ν, the period-doubling bifurcation and Neimark-Sacker bifurcation at the equilibrium point P_7 of the controlled system (7.9) can be either accelerated, postponed, or completely removed. The Jacobian matrix of the controlled system (7.9), evaluated at P_7, is expressed as follows:

$$J_*(L_7,G_7) = \begin{bmatrix} 1-\nu H\left(3aL_7^2-(2a(b+1)-c)L_7+a_0b+ce\right) & -cL_7\nu H \\ \frac{\nu H}{d+e+L_7} & 1-\frac{\nu H}{d+e+L_7} \end{bmatrix}. \tag{7.10}$$

The characteristic equation corresponding to the Jacobian matrix $J_*(P_7)$ is

$$F_*(\xi)=\xi^2+r_*\xi+s_*=0,$$

where

$$r_*=-2+g_7\nu H,\quad s_*=1-g_7\nu H+k_7\nu^2H^2.$$

For the stability of the system (7.9), $F_*(1)>0$, $F_*(-1)>0$ and $F_*(0)<0$, where

$$\begin{aligned} F_*(1)>0 &\Rightarrow k_7\nu^2H^2>0,\\ F_*(-1)>0 &\Rightarrow 4-2g_7\nu H+k_7\nu^2H^2>0,\\ F_*(0)<0 &\Rightarrow 1-g_7\nu H+k_7\nu^2H^2<0. \end{aligned}$$

The following lemma establishes the conditions for the local asymptotic stability of P_7 in the controlled system (7.9).

Lemma 3. *The positive equilibrium P_7 of the controlled system* (7.9) *is locally asymptotically stable provided that the following conditions are satisfied:*

$$k_7\nu^2 > 0, \quad 4 - 2g_7\nu H + k_7\nu^2H^2 > 0, \quad 1 - g_7\nu H + k_7\nu^2H^2 < 0.$$

For $\nu \in (0.5, 1)$, the system (7.9) is stable at fixed point P_7. Figure 6(a) depicts a bifurcation diagram which shows periodic solution in the system. If we compare it with Figure 6(b)–(e), it is easily seen that the chaos has been reduced to the periodic windows.

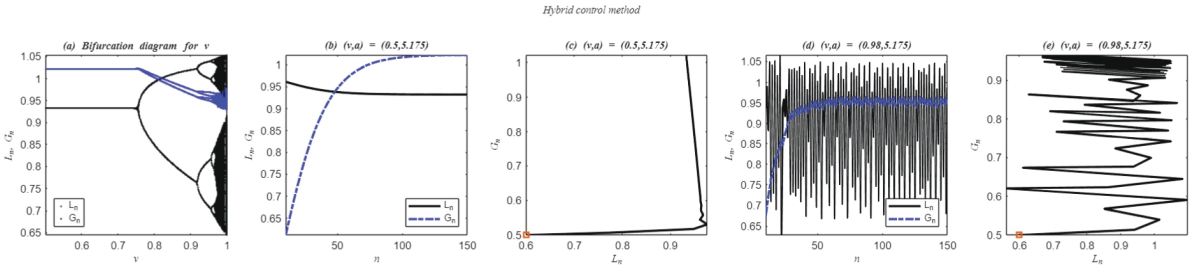

Figure 6. (a) Bifurcation for the hybrid parameter ν. (b)–(e) Phase portraits of the system (7.9) inside and outside the stability interval for ν, where the red circle refers to the initial condition.

7.3. State feedback control

State feedback control provides an optimal approach to managing chaotic systems [42]. This technique transforms the chaotic system into a piecewise linear system through the use of an optimal controller. It reduces the upper bound and, under specific conditions, enables control within the system. By applying an appropriate control mechanism, the resulting controlled system derived from (2.10) is expressed as follows:

$$\begin{aligned} L_{n+1} &= L_n + H\left[aL_n\left(1 - L_n\right)\left(L_n - b\right) - cL_nG_n\right] + j_1(L_n - L_7) + j_2(G_n - G_7), \\ G_{n+1} &= G_n + H\left[\frac{G_n}{d + G_n}\left(1 - \frac{G_n}{e + L_n}\right)\right]. \end{aligned} \tag{7.11}$$

This represents the desired control force under the feedback control law, where j_1 and j_2 are the feedback gains. The Jacobian matrix of the system (7.11) yields the following characteristic equation:

$$F_s(\xi) = \xi^2 + (\xi_{s1} + \xi_{s2})\xi + \xi_{s1}\xi_{s2} = 0, \tag{7.12}$$

where

$$\begin{aligned} \xi_{s1} + \xi_{s2} &= (g_7H - j_1 - 2), \\ \xi_{s1}\xi_{s2} &= k_7H^2 - \left(\frac{j_1 + j_2 + 1}{d + e + L_7} + 3aL_7^2 - (2a\left(b + 1\right) - c)\,L_7 + ab + ce\right)H + j_1 + 1, \end{aligned}$$

and ξ_{s1} and ξ_{s2} are two solutions of the characteristic Eq (7.12).

The conditions defining the marginal stability lines are now provided as follows:

$$\xi_{s1} = \pm 1, \;\; \xi_{s1}\xi_{s2} = 1,$$

For the second condition, Eq (7.12) provides

$$L_{s1} : k_7 H^2 - \left(\frac{j_1 + 1}{d + e + L_7} + (j_2 + 1)\left(3aL_7^2 - (2a\,(b + 1) - c)\,L_7 + ab + ce\right)\right) H + (j_2 + 1)j_1 + j_2 = 0, \tag{7.13}$$

For another condition of stability, if $\xi_{s1} = 1$ we get

$$L_{s2} : k_7 H^2 - \left(\frac{j_1}{d + e + L_7} + \left(3aL_7^2 - (2a\,(b + 1) - c)\,L_7 + ab + ce\right) j_2\right) H + j_1 j_2 = 0. \tag{7.14}$$

Similarly for $\xi_{s1} = -1$, it is seen that

$$L_{s3} : k_7 H^2 - \left(\frac{j_1 + 2}{d + e + L_7} + \left(3aL_7^2 - (2a\,(b + 1) - c)\,L_7 + ab + ce\right) (j_2 + 2)\right) H + (j_2 + 2)(j_1 + 2) = 0. \tag{7.15}$$

For stability, all eigenvalues must lie within the stability region defined by the lines L_{s1}, L_{s2}, and L_{s3}. Thus, it can be inferred that the system (7.11) is stable if its corresponding eigenvalues fall within the open unit disk.

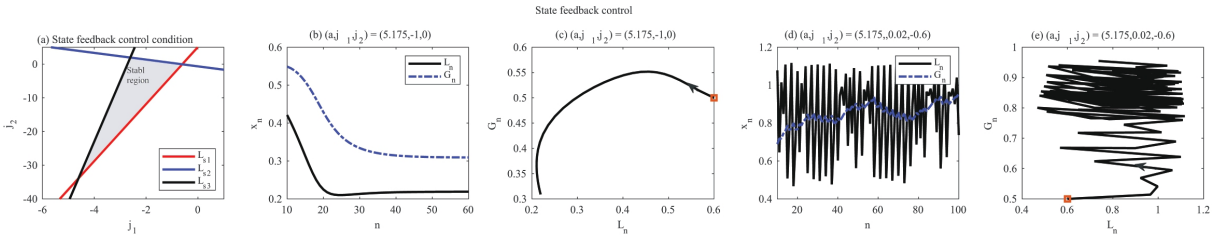

Figure 7. (a) State feedback control condition. (b)–(e) Phase portraits of the system (7.11) inside and outside the stability region bounded by L_{s1}, L_{s2}, and L_{s3}), the red circle refers to the initial condition.

In practical terms, chaos control provides a framework for managing real-world ecological challenges. It informs strategies for stabilizing endangered species by guiding populations away from erratic fluctuations, supports the design of sustainable harvesting policies that prevent resource depletion, and enhances biological pest control by enabling targeted interventions that maintain pest populations below economic thresholds without disrupting the ecosystem.

8. Conclusions

This research presents a discrete-time Leslie-Gower predator-prey model that uses fractional-order dynamics with constant parameters. Fractional order incorporates ecological memory (delayed maturation, resource regeneration), enhancing the realism of predictions and providing an extra management tool. We looked at the existence of both disease-free and positive equilibrium states and checked how stable they were in the area. We examined the Neimark-Sacker and flip bifurcations

of the system defined by the model (2.1) through the application of the center manifold theorem and bifurcation theory. Our study demonstrates that the model exhibits intricate dynamic characteristics, including Neimark-Sacker and flip bifurcations. We discovered phenomena such as period-doubling sequences (periods 2, 4, 8, 24) and chaotic attractors. The maximal Lyapunov exponent was utilized to discover behavior that was chaotic. We investigate the influence of environmental conditions on the ecosystem's stability to enhance our comprehension of predator-prey dynamics. A discrete-time fractional-order modified Leslie-Gower predator-prey model is used to look at two important ecological events. The Allee effect says that low-density conditions lower fitness, which could lead to a decline in prey numbers. Fear alters the behavior and physiology of prey, influencing predators' success and ecological dynamics. To elucidate the intricate behaviors of this model, we use two-parameter dynamics, encompassing Lyapunov diagram creation and the determination of the greatest Lyapunov exponent. These techniques provide a systematic investigation of the parameter space to identify chaotic regions and stability transitions. Parameters like growth rates, carrying capacities, and the intensity of Allee and fear intensities determine how the model changes over time. This helps us comprehend the difference between chaos and stability. This helps us understand how predators and prey interact and how outside factors affect the stability of the ecosystems.

Future research will enhance the model to incorporate ecological complexities, including stochastic changes and regional heterogeneity. Due to the inherent chaos of ecosystems, achieving accurate forecasts remains challenging. Future research could use data-driven methodologies to enhance predictive accuracy. Examining the influence of bifurcation patterns on the likelihood of a population's survival or extinction is also crucial.

Author contributions

Abdulaziz Almaslokh: Conceptualization, formal analysis, writing-review & editing, critical review; Ibrahim M. E. Abdelstar: Conceptualization, formal analysis, graphic, drawing writing-review & editing, critical review; A. A. Elsadany: Methodology; formal analysis, writing-review & editing. All authors have read and approved the final version of the manuscript for publication.

Use of Generative-AI tools declaration

The authors declare they have not used artificial intelligence (AI) tools in the creation of this article.

Acknowledgments

The authors extend their appreciation to Prince Sattam bin Abdulaziz University for funding this research work through project number (PSAU/2025/01/37224).

Conflicts of interest

The authors declare no conflicts of interest.

References

1. A. Das, G. P. Samanta, A prey–predator model with refuge for prey and additional food for predator in a fluctuating environment, *Physica A*, **538** (2020), 122844. https://doi.org/10.1016/j.physa.2019.122844
2. M. El-Shahed, A. M. Ahmed, I. M. Abdelstar, A fractional-order model for the spread of pests in tea plants, *Adv. Anal.*, **1** (2016), 68–79. https://doi.org/10.22606/aan.2016.12002
3. M. El-Shahed, A. M. Ahmed, I. M. E. Abdelstar, Dynamics of a plant-herbivore model with fractional order, *Prog. Fract. Differ. Appl.*, **53** (2017), 59–67. https://doi.org/10.18576/pfda/030106
4. F. A. Rihan, *Delay differential equations and applications to biology*, Springer, 2021.
5. M. A. A. Alaoui, M. D. Okiye, Boundedness and global stability for a predator-prey model with modified leslie-gower and holling-type ii schemes, *Appl. Math. Lett.*, **16** (2003), 1069–1075. https://doi.org/10.1016/S0893-9659(03)90096-6
6. M. A. A. Alaoui, Study of a leslie–gower-type tritrophic population model, *Chaos Soliton. Fract.*, **14** (2002), 1275–1293. https://doi.org/10.1016/S0960-0779(02)00079-6
7. E. G. Olivares, J. M. Lorca, A. R. Palma, J. D. Flores, Dynamical complexities in the leslie–gower predator–prey model as consequences of the allee effect on prey, *Appl. Math. Model.*, **35** (2011), 366–381. https://doi.org/10.1016/j.apm.2010.07.001
8. M. M. Chen, Y. Takeuchi, J. F. Zhang, Dynamic complexity of a modified leslie–gower predator–prey system with fear effect, *Commun. Nonlinear Sci.*, **119** (2023), 107109. https://doi.org/10.1016/j.cnsns.2023.107109
9. Y. L. Xue, Impact of both-density-dependent fear effect in a leslie–gower predator–prey model with beddington–deangelis functional response, *Chaos Soliton. Fract.*, **185** (2024), 115055. https://doi.org/10.1016/j.chaos.2024.115055
10. C. G. Dittmer, Animal aggregations: A study in general sociology, 1931.
11. B. Dennis. Allee effects: population growth, critical density, and the chance of extinction. *Nat. Resour. Model.*, **3** (1989), 481–538. https://doi.org/10.1111/j.1939-7445.1989.tb00119.x
12. A. M. Kramer, B. Dennis, A. M. Liebhold, J. M. Drake, The evidence for allee effects, *Popul. Ecol.*, **51** (2009), 341–354. https://doi.org/10.1007/s10144-009-0152-6
13. Q. Q. Fang, X. Y. Li, Complex dynamics of a discrete predator–prey system with a strong allee effect on the prey and a ratio-dependent functional response, *Adv. Differ. Equ.*, **2018** (2018), 320. https://doi.org/10.1186/s13662-018-1781-x
14. E. G. Olivares, A. R. Palma, B. G. Yañez, Multiple limit cycles in a leslie–gower-type predator–prey model considering weak allee effect on prey, *Nonlinear Anal.-Model.*, **22** (2017), 347–365. https://doi.org/10.15388/NA.2017.3.5
15. L. Berec, E. Angulo, F. Courchamp, Multiple allee effects and population management, *Trends Ecol. Evol.*, **22** (2007), 185–191. https://doi.org/10.1016/j.tree.2006.12.002
16. S. Eggers, M. Griesser, M. Nystrand, J. Ekman, Predation risk induces changes in nest-site selection and clutch size in the siberian jay, *P. Roy. Soc. B-Biol. Sci.*, **273** (2006), 701–706. https://doi.org/10.1098/rspb.2005.3373

17. S. Creel, D. Christianson, Relationships between direct predation and risk effects, *Trends Ecol. Evol.*, **23** (2008), 194–201. https://doi.org/10.1016/j.tree.2007.12.004

18. K. Chen, *Analysis of arousal and valence based on eeg signals: Research on emotional analysis*, In: Proceedings of the 2023 12th International Conference on Bioinformatics and Biomedical Science, 2023, 59–68. https://doi.org/10.1145/3647817.3647826

19. R. C. Wu, W. K. Xiong, Bifurcation in a leslie–gower system with fear in predators and strong allee effect in prey, *Nonlinear Anal.-Model*, **30** (2025), 1–18. https://doi.org/10.15388/namc.2025.30.38982

20. M. F. Elettreby, Two-prey one-predator model, *Chaos Soliton. Fract.*, **39** (2009), 2018–2027. https://doi.org/10.1016/j.chaos.2007.06.058

21. B. J. West, *Nature's patterns and the fractional calculus*, Walter de Gruyter GmbH & Co KG, **2** (2017).

22. J. T. Machado, V. Kiryakova, F. Mainardi, Recent history of fractional calculus, *Commun. Nonlinear Sci.*, **16** (2011), 1140–1153. https://doi.org/10.1016/j.cnsns.2010.05.027

23. C. Ionescu, A. Lopes, D. Copot, J. A. T. Machado, J. H. T. Bates, The role of fractional calculus in modeling biological phenomena: A review, *Commun. Nonlinear Sci.*, **51** (2017), 141–159. https://doi.org/10.1016/j.cnsns.2017.04.001

24. V. E. Tarasov, On history of mathematical economics: Application of fractional calculus, *Mathematics*, **7** (2019), 509. https://doi.org/10.3390/math7060509

25. Y. W. Jiang, B. Zhang, *Comparative study of riemann–liouville and caputo derivative definitions in time-domain analysis of fractional-order capacitor*, In: IEEE Transactions on Circuits and Systems II: Express Briefs, **67** (2019), 2184–2188. https://doi.org/10.1109/TCSII.2019.2952693

26. K. M. Owolabi, A. Atangana, A. Akgul, Modelling and analysis of fractal-fractional partial differential equations: Application to reaction-diffusion model, *Alex. Eng. J.*, **59** (2020), 2477–2490. https://doi.org/10.1016/j.aej.2020.03.022

27. H. M. Srivastava, Fractional-order derivatives and integrals: Introductory overview and recent developments, *Kyungpook Math. J.*, **60** (2020), 73–116. https://doi.org/10.5666/KMJ.2020.60.1.73

28. A. A. Elsadany, A. E. Matouk, Dynamical behaviors of fractional-order lotka–volterra predator–prey model and its discretization, *J. Appl. Math. Comput.*, **49** (2015), 269–283. https://doi.org/10.1007/s12190-014-0838-6

29. M. El-Shahed, I. M. E. Abdelstar, Stability and bifurcation analysis in a discrete-time sir epidemic model with fractional-order, *Int. J. Nonlin. Sci. Num.*, **20** (2019), 339–350. https://doi.org/10.1515/ijnsns-2018-0088

30. F. A. Rihan, S. Lakshmanan, A. H. Hashish, R. Rakkiyappan, E. Ahmed, Fractional-order delayed predator–prey systems with holling type-ii functional response, *Nonlinear Dynam.*, **80** (2015), 777–789. https://doi.org/10.1007/s11071-015-1905-8

31. B. K. Lenka, S. N. Bora, New comparison results for nonlinear caputo-type real-order systems with applications, *Nonlinear Dynam.*, **111** (2023), 19249–19264. https://doi.org/10.1007/s11071-023-08846-4

32. J. Alidousti, M. M. Ghahfarokhi, Dynamical behavior of a fractional three-species food chain model, *Nonlinear Dynam.*, **95** (2019), 1841–1858. https://doi.org/10.1007/s11071-018-4663-6
33. A. M. Yousef, S. Z. Rida, Y. G. Gouda, A. S. Zaki, Dynamical behaviors of a fractional-order predator–prey model with holling type iv functional response and its discretization, *Int. J. Nonlin. Sci. Num.*, **20** (2019), 125–136. https://doi.org/10.1515/ijnsns-2017-0152
34. U. Ghosh, S. Pal, M. Banerjee, Memory effect on bazykin's prey-predator model: Stability and bifurcation analysis, *Chaos Soliton. Fract.*, **143** (2021), 110531. https://doi.org/10.1016/j.chaos.2020.110531
35. J. Alzabut, A. G. M. Selvam, V. Dhakshinamoorthy, H. Mohammadi, S. Rezapour, On chaos of discrete time fractional order host-immune-tumor cells interaction model, *J. Appl. Math. Comput.*, **68** (2022), 4795–4820. https://doi.org/10.1007/s12190-022-01715-0
36. A. E. Matouk, A. A. Elsadany, Dynamical analysis, stabilization and discretization of a chaotic fractional-order glv model, *Nonlinear Dynam.*, **85** (2016), 1597–1612. https://doi.org/10.1007/s11071-016-2781-6
37. A. E. Matouk, A. A. Elsadany, E. Ahmed, H. N. Agiza, Dynamical behavior of fractional-order hastings–powell food chain model and its discretization, *Commun. Nonlinear Sci.*, **27** (2015), 153–167. https://doi.org/10.1016/j.cnsns.2015.03.004
38. N. Song, Bifurcation and chaos of a nonlinear discrete-time predator-prey model involving the nonlinear allee effect, *Discrete Dyn. Nat. Soc.*, **2023** (2023), 5475999. https://doi.org/10.1155/2023/5475999
39. S. N. Elaydi, *Discrete chaos: With applications in science and engineering*, Chapman and Hall/CRC, 2007.
40. S. N. Elaydi, *An introduction to difference equations*, Berlin: Springer, 2005.
41. E. Ott, C. Grebogi, J. A Yorke, Controlling chaos, *Phys. Rev. Lett.*, **64** (1990), 2837. https://doi.org/10.1103/PhysRevLett.64.2837
42. Q. Din, Complexity and chaos control in a discrete-time prey-predator model, *Commun. nonlinear Sci.*, **49** (2017), 113–134. https://doi.org/10.1016/j.cnsns.2017.01.025
43. L. G. Yuan, Q. G. Yang, Bifurcation, invariant curve and hybrid control in a discrete-time predator–prey system, *Appl. Math. Model.*, **39** (2015), 2345–2362. https://doi.org/10.1016/j.apm.2014.10.040